Acta Cryst. (1959). **12**, 360

The Scattering of Electrons by Atoms and Crystals. III. Single-Crystal Diffraction Patterns

BY J. M. COWLEY AND A. F. MOODIE

Division of Chemical Physics, Chemical Research Laboratories, Commonwealth Scientific and Industrial Research Organization, Melbourne, Australia

(*Received* 12 *May* 1958)

Some aspects of the diffraction of electrons by single crystals are discussed using low-order approximations to the general theory developed in the first paper of this series (Cowley & Moodie, 1957) and some qualitative arguments concerning general results are presented.

The first-order approximation involves the treatment of a crystal as a phase object for electrons. This leads to a complex form for the atomic scattering factor and the structure factor which introduces complications to, but opens up new possibilities for, the process of structure analysis from single-crystal electron diffraction patterns.

It is shown that forbidden reflections cannot be generated by dynamic scattering effects in the symmetrical spot patterns obtained when the electron beam is parallel to a principal crystal axis, but lattice defects can give rise to forbidden reflections in such patterns from thick crystals.

1. Introduction

In the first paper of this series (Cowley & Moodie, 1957; hereafter referred to as I) there was described a general theory of the scattering of electron waves by the potential fields of atoms and crystals, based on the new formulation of physical optics recently presented (Cowley & Moodie, 1958). The effect on the electron wave function of a three-dimensional potential field was approximated by the effect of a large number of closely spaced two-dimensional potential fields.

In particular, expressions were derived for the amplitude distributions in the diffraction pattern of a crystal assumed to be of infinite extent and perfectly periodic in directions perpendicular to the incident electron beam, the diffraction pattern being defined as the angular distribution of scattered amplitude at infinity, or the positional distribution on the back focal plane of an ideal thin lens, for perfectly coherent and parallel incident radiation. In the second paper of this series (Cowley & Mcodie, 1959) it was shown that, provided excessively large electron sources are not employed, the diffraction pattern from such a crystal is independent of the coherence properties of the incident radiation and has an intensity distribution given by convolution of the diffracted intensity distribution for a point source with the intensity distribution of the source, suitably scaled. It is therefore sufficient for our purposes to consider only the point-source diffraction patterns.

In the present paper we consider in greater detail the diffraction patterns given by such extensive thin crystals and derive some results of interest for practical electron diffraction investigations. In particular we consider the extensive patterns of spots given by very thin single crystals when the incident electron beam is perpendicular to a principal plane of the reciprocal lattice. Such patterns have been used as the basis for crystal structure analysis (Cowley, 1953).

The principal limitation to their use in this way is that at present the techniques of specimen preparation are not sufficiently developed to ensure that the thickness of the crystals used is always less than the limiting thickness beyond which the kinematic theory of electron diffraction ceases to be an adequate approximation. On the other hand no adequate theoretical treatment has been available to indicate the way in which the diffraction patterns may be modified when the thickness exceeds this limit and dynamic scattering effects become appreciable. The original dynamic theory of Bethe has been applied only to cases where two, three and, to a limited extent, four strong beams exist in the crystal simultaneously (see, for example, Heidenreich, 1950). It would appear that the theory outlined in I allows a new and probably more fruitful approach to the case of dynamic scattering for the large number of simultaneous reflections given by relatively thin crystals.

We employ the methods of approximation which were discussed in I. Firstly, the amplitude scattered in any direction may be expressed as the sum of contributions from electrons scattered $1, 2, 3 \ldots n$ times. For crystals which are not too thick in the beam direction these contributions form the terms of a rapidly convergent series. Secondly, the three-dimensional potential distribution may be approximated by a number of two-dimensional distributions, appropriately spaced. The approximation improves as the number of two-dimensional distributions is increased.

2. First-order approximations

When we consider the scattering of electrons through angles of only a few degrees by a potential field which is of very small extent in the beam direction, the effect of the potential field on the electron beam may be approximated by the effect of a single two-dimensional potential distribution on a plane perpendicular to the beam, given by

$$\varphi(x, y) = \int_{-\infty}^{\infty} \varphi(x, y, z) . dz \, , \qquad (1)$$

where the beam is assumed to be parallel to the z-axis.

If we neglect the term $\chi(x, y)$ which appears in I, representing the decrease in amplitude due to inelastic scattering of electrons, the effect of the potential field on the electron wave function is a phase change represented by a factor

$$q_1(x, y) = \exp \{i\sigma\varphi(x, y)\} \, , \qquad (2)$$

where σ is a constant equal to $2\pi m\lambda/h^2$.

The corresponding diffraction patterns are then given by the Fourier transform of $q_1(x, y)$, as

$$\begin{aligned} U(u, v) &= \mathfrak{F}\,[\exp \{i\sigma\varphi(x, y)\}] \\ &= \mathfrak{F}\,[\cos \sigma\varphi(x, y)] + i\mathfrak{F}\,[\sin \sigma\varphi(x, y)] \, . \end{aligned} \qquad (3)$$

This is the approximation discussed in section 7(a) of I. Apart from the fact that the Ewald sphere is replaced by a plane, this approximation goes beyond the ordinary kinematic theory of diffraction in that it takes account of the phase nature of the scattering material, but does not include the full range of dynamic scattering effects in that it ignores the Fresnel diffraction effects operating when the crystal has finite thickness to spread the influence of each atom on the electron wave over an increased area of the exit face.

This approximation should be very good if scattering by individual atoms, rather than crystals, is considered since then the Ewald sphere curvature and multiple scattering effects should not influence the scattering distribution appreciably. The diffraction pattern in this case corresponds to the atomic scattering factor which, from (3), is given by

$$\begin{aligned} g(u, v) &= \mathfrak{F}\,[\exp \{i\sigma\varphi(x, y)\}] \\ &= \delta(u, v) + i\sigma g^B(u, v) - \tfrac{1}{2}\sigma^2 \{g^B(u, v) * g^B(u, v)\} - \ldots \, , \end{aligned} \qquad (4)$$

where the δ-function represents the incident beam and $g^B(u, v)$ is the atomic scattering factor in the kinematic approximation as given by the first Born approximation in quantum-mechanical scattering theory. The atomic scattering factor so defined is obviously complex. It is readily shown that its behaviour is qualitatively the same as that of the complex atomic scattering factors derived by Schomaker & Glauber (1952) using the second Born approximation and those of Ibers & Hoerni (1954) who used the partial waves scattering theory. The phase angle increases with the atomic number of the atom, the scattering angle and the electron wave length. A quantitative comparison of the values of $g(u, v)$ from (3) with those calculated by Ibers & Hoerni (1954) is being made and may be published shortly.

Schomaker & Glauber (1952) pointed out that the kinematic approximation may not be sufficiently accurate for electron diffraction work when scattering from both heavy and light atoms is involved. When scattering by crystals is considered, the maximum values of $\varphi(x, y)$ as defined by (1) will be greater than that for a single atom by a factor equal to the number of atoms exactly in line in the beam direction. We must therefore reject the kinematic approximation even for very thin crystals when a wide range of atomic numbers is involved, and use as a first approximation the analogue of (4) for periodic $\varphi(x, y)$, thus

$$\begin{aligned} U(h, k) &= \mathfrak{F}\,[\exp \{i\sigma\varphi(x, y)\}] \\ &= \delta(h, k) + i\sigma E(h, k) - \frac{\sigma^2}{2} \{E(h, k) * E(h, k)\} - \ldots \, , \end{aligned} \qquad (5)$$

where $E(h, k)$ is the kinematic structure factor.

From (3) the scattering amplitude is given by the sum of the transforms of a cosine and a sine term, both of which will be complex unless $\varphi(x, y)$ has a centre of symmetry. The function $\cos \sigma\varphi(x, y)$ may be considered as the sum of a centrosymmetric function $\frac{1}{2}[\cos \sigma\varphi(x, y) + \cos \sigma\varphi(-x, -y)]$ and an anti-centrosymmetric function

$$\tfrac{1}{2}[\cos \sigma\varphi(x, y) - \cos \sigma\varphi(-x, -y)] \, .$$

The Fourier transforms of these two functions may be written $C_{\cos}$ and $iA_{\cos}$ respectively. For the sine function we define, similarly, $C_{\sin}$ and $iA_{\sin}$.

Then

$$\begin{aligned} U(h, k) &= C_{\cos} + iA_{\cos} + i(C_{\sin} + iA_{\sin}) \\ &= (C_{\cos} - A_{\sin}) + i(C_{\sin} + A_{\cos}) \, . \end{aligned}$$

The intensities of the diffraction spots will be proportional to

$$I(h, k) = |U(h, k)|^2 = (C_{\cos} - A_{\sin})^2 + (C_{\sin} + A_{\cos})^2 \, .$$

If the indices h, k be replaced by $-h, -k$, the signs of the $A_{\sin}$ and $A_{\cos}$ will be reversed, so that

$$I(-h, -k) = (C_{\cos} + A_{\sin})^2 + (C_{\sin} - A_{\cos})^2 \, .$$

For non-centrosymmetric structures, therefore, the intensity distribution in the diffraction pattern is not symmetric about the origin.

For convenience, we limit our considerations to centrosymmetric crystals, for which the intensity of the diffraction spots will be proportional to

$$I(h, k) = \{\mathfrak{F}\,[\cos \sigma\varphi(x, y)]\}^2 + \{\mathfrak{F}\,[\sin \sigma\varphi(x, y)]\}^2 \, .$$

If such intensities were to be used for purposes of structure analysis of the crystal, the first step would be to calculate the Patterson function, given by

$$\begin{aligned} P(x, y) = {} & [\{\cos \sigma\varphi(x, y)\} * \{\cos \sigma\varphi(-x, -y)\}] \\ & + [\{\sin \sigma\varphi(x, y)\} * \{\sin \sigma\varphi(-x, -y)\}] \, . \end{aligned} \qquad (6)$$

This is to be compared with the normal kinematic Patterson function

$$P_{\text{kin}}(x, y) = \sigma\varphi(x, y) * \sigma\varphi(-x, -y) . \qquad (7)$$

In order to gain some impression of the modification of the Patterson function represented by (6), we have calculated the peak shapes which would be obtained for Gaussian atoms of constant width but variable height, i.e., taking

$$\sigma\varphi(x, y) = c \exp(-x^2)$$

with values of c from 1·0 to 8·0 to represent variations in the atomic number of the atoms or the crystal thickness. In Fig. 1 are shown the peak shapes for one-dimensional Patterson peaks corresponding to vectors between identical Gaussian atoms, obtained by graphical evaluation of the convolutions

$$\cos\{c \exp(-x^2)\} * \cos\{c \exp(-x^2)\} \quad \text{and} \quad \sin\{c \exp(-x^2)\} * \sin\{c \exp(-x^2)\}$$

for various values of c. The way in which the peak heights and the total areas of the peaks vary with c is given by the curves of Fig. 2.

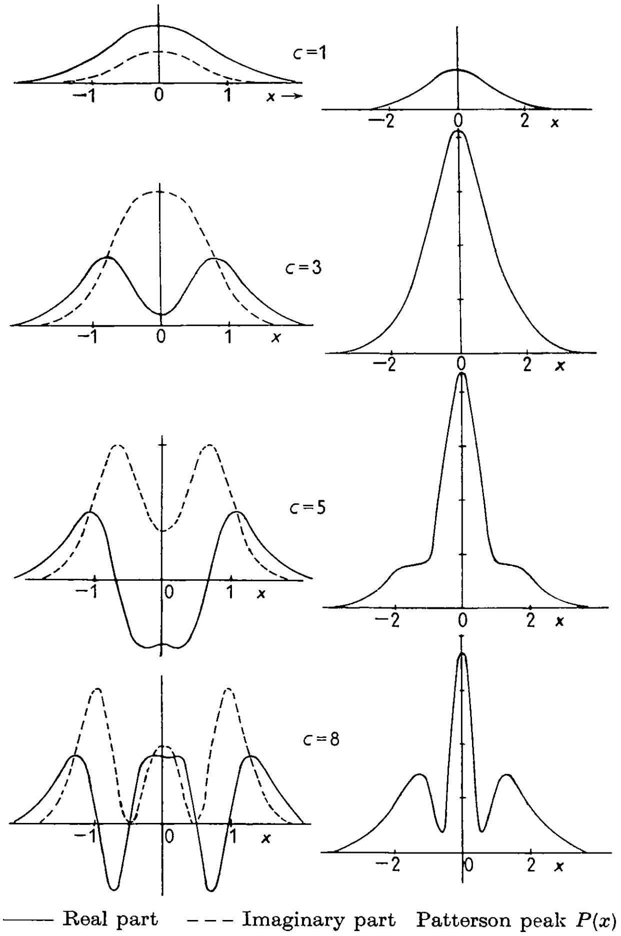

Fig. 1. The real and imaginary parts of the function $\exp\{ic \exp(-x^2)\}$ and the Patterson peak given by the convolution $\exp\{ic \exp(-x^2)\} * \exp\{-ic \exp(-x^2)\}$ for $c = 1, 3, 5$ and 8.

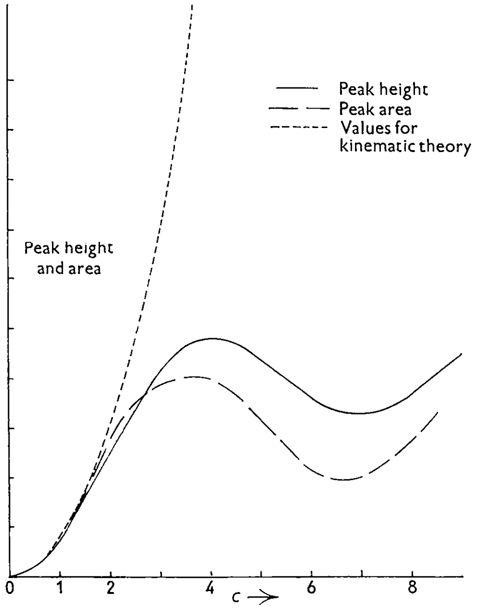

Fig. 2. The variation with c of the peak height (continuous line) and peak area (dashed line) for Patterson peaks similar to those shown in Fig. 1, compared with the variation of the peak height and area (dotted line) given by the kinematic theory. The ordinates have been adjusted so that the kinematic peak height and peak area curves coincide.

It is seen that the peaks of the Patterson map given by (6) differ appreciably from those of the kinematic Patterson map, given by (7), for values of c greater than about 2. Relative to the kinematic Patterson peaks, the peaks decrease in height and also in width as c increases. Subsidiary peaks appear for c greater than 5 and slowly increase in number and in size relative to the central peak as c increases further.

The order of magnitude of such effects in practice can be appreciated as a result of rough calculations which give $c \approx 1$ for a single uranium atom and $c \approx 0{\cdot}1$ for a single carbon atom. If there are n atoms superimposed in the direction of the beam, the effects obtained correspond to putting $c = n$ for uranium atoms or $c = n/10$ for carbon atoms.

In Fig. 3(*a*) and (*b*) are plotted the peak shapes corresponding to vectors between unequal Gaussian atoms represented by

$$\exp\{ic_1 \exp(-x^2)\} \quad \text{and} \quad \exp\{ic_2 \exp(-x^2)\}.$$

In Fig. 3(*a*), $c_1 = 0{\cdot}5$, and c_2 is varied from 1·0 to 6. In Fig. 3(*b*), $c_1 = 1{\cdot}0$ and c_2 is varied from 1·0 to 6.

It thus appears that, in extreme cases, the central parts of Patterson peaks corresponding to vectors between atoms of widely different atomic number may be very much reduced in height and may even become negative.

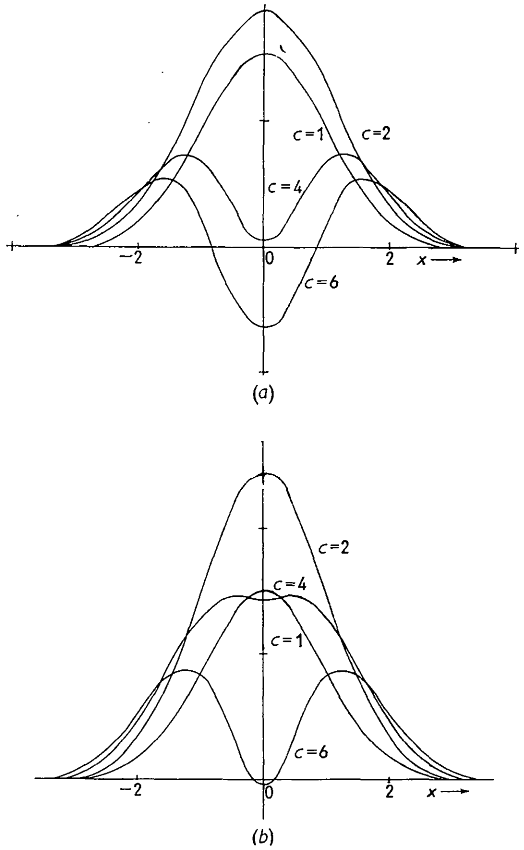

Fig. 3. The Patterson peak shapes given by evaluating the convolutions

$$\cos\{c_1 \exp(-x^2)\} * \cos\{c_2 \exp(-x^2)\} \quad \text{and}$$
$$\sin\{c_1 \exp(-x^2)\} * \sin\{c_2 \exp(-x^2)\}\,.$$

For 3(*a*): $c_1 = \frac{1}{2}$, $c_2 = 1, 2, 4$ and 6.
For 3(*b*): $c_1 = 1$, $c_2 = 1, 2, 4$ and 6.

We now make the plausible assumption that the results obtained for one-dimensional Gaussian atoms may be applied to give at least a qualitative indication of the equivalent results for real three-dimensional atoms or their two-dimensional projections, and proceed to consider how the failure of the kinematic scattering approximation may affect the processes of the structure analysis of crystals. For thin crystals in which the deviations from kinematic scattering are not excessive, it is evident that the principal effect on the form of Patterson maps will be that the peaks representing interactions between heavy atoms will be reduced in height and diameter while peaks representing interactions between light atoms may not be appreciably affected. Peaks from light-heavy atom interactions may be somewhat broadened and flattened. However, the positions of the peaks will remain unchanged, and, provided that peak heights can be correctly interpreted, an examination of the Patterson maps may lead to a correct determination of the crystal structure.

If electron diffraction patterns could be obtained from crystals of one substance with several different known thicknesses, it would be possible to confirm the predictions as to the variation of Patterson peak shape. It would be possible to extrapolate to zero thickness and so obtain the true kinematic Patterson map and intensity distribution. Further, the dependence of the peak shape and its variation with crystal thickness on the nature of the atom pairs involved in its production would allow techniques of structure analysis to be developed leading to an unambiguous structural determination directly from experimental data. These techniques would be similar to those involving the use of anomalous X-ray scattering, since in each case advantage is taken of a controlled change in the relative phases of scattering by atoms of differing atomic number.

If sufficient was known of a structure to allow at least one Patterson peak to be definitely identified as being given by atom pairs of a given type, the form of this peak could be used to establish a scale of thickness. It would then be unnecessary to make thickness measurements on all crystals used.

An alternative to varying the crystal thickness would be to vary the wavelength, i.e., the accelerating voltage, of the incident beam. This would have the advantage that all patterns could be obtained from the same crystal, held in the same orientation with respect to the electron beam. Usually, also, measurements of accelerating voltage may be made more conveniently and accurately than measurements of crystal thickness in the ranges which would be employed. However, the range of accelerating voltage desirable for successful extrapolation to zero wavelength may be considerable, since σ is proportional to $W_0^{-\frac{1}{2}}$.

The above results have been based on assumptions which limit their direct application to practical problems. By approximating to a crystal by a single two-dimensional distribution of potential, the curvature of the Ewald sphere has been ignored. This approximation is satisfactory for the electron wavelengths normally employed only for very thin crystals or for diffraction spots not too far from the origin. If patterns could be obtained for wavelengths much shorter than that for 50 kV. electrons, the extrapolation process used to correct for dynamic scattering effects would also correct for the effect of the finite radius of curvature of the Ewald sphere, although the latter effect may reduce the accuracy of the extrapolation process.

If the crystal is approximated to by two two-dimensional potential distributions, rather than one, the influence of the curvature of the Ewald sphere is introduced in part along with the effect of the Fresnel diffraction between distributions, and approximation by a greater number of two-dimensional potential distributions introduces the effect of the curvature in a progressively more accurate form. Such higher approximations may be calculated following section 7 of I, but do not appear to introduce any novel features of general interest and so will not be treated in detail here.

A further assumption which has been made is that the crystal is perfect. This is rarely true in practice. Experience has shown that small crystals, in the range of sizes useful for electron diffraction work, frequently show a considerable amount of disorder, often in the form of stacking defects. The effects of one or more stacking defects on the diffraction pattern produced will be discussed in a subsequent section.

3. The appearance of 'forbidden' reflections

'Forbidden' reflections are those for which the structure factor in the kinematic diffraction theory is zero as a result of the space-group symmetry of the crystal structure. When, however, the indices of a 'forbidden' reflection can be expressed in the form h_1+h_2, k_1+k_2, l_1+l_2, where h_1, k_1, l_1 and h_2, k_2, l_2 are indices of allowed reflections, it is frequently observed that the forbidden reflections in electron diffraction spot patterns occur with appreciable intensity. This is usually interpreted as being the result of dynamic scattering. Heidenreich (1950), for example, explained the appearance of the 'forbidden' (222) reflection from a diamond-type lattice as arising from dynamic interaction of diffracted beams by applying Bethe's dynamic theory to the case that only three strong beams exist in the crystal lattice. It has been assumed that, if a similar treatment of the case of many strong beams were possible, it would similarly lead to the prediction of forbidden reflections in the extensive, symmetrical spot patterns obtained when the incident beam is parallel to a principal lattice axis of a thin crystal. Our present approach to dynamic diffraction theory allows us to treat this case with greater facility and demonstrate that such an assumption is not justified.

The effect on an incident electron wave of a parallel-sided crystal plate which may be assumed of infinite extent in directions perpendicular to the beam, may be approximated by the effect of a large number, N, of two-dimensional potential distributions, $\varphi_n(x, y)$, spaced at intervals $\Delta z = H/(N-1)$, where H is the crystal thickness. The approximation may be made as good as required by taking N sufficiently large. In particular if N is made equal to the number of unit cells of the crystal lattice in the beam direction the approximation will be sufficiently good for all practical purposes unless the unit-cell dimension is very large (i.e., hundreds of Ångströms under normal diffraction conditions). Then all the $\varphi_n(x, y)$ will be identical, each representing the projection of the potential distribution of one unit-cell thickness.

For a plane-parallel incident beam normal to the crystal face, the wave function on the exit face of the crystal is then given by the formulation of Cowley & Moodie (1958) as

$$\begin{aligned}\psi(x, y) = q_N(x, y)\Big[_{N-1}\, q_{N-1}(x, y)\ldots\Big[_2\, q_2(x, y)\\ \times \Big[_1\, q_1(x, y) * p_1(x, y)\Big]_1 * p_1(x, y)\Big]_2 * \ldots\\ \ldots * p_1(x, y)\Big]_{N-1},\end{aligned} \tag{8}$$

where $p_1(x, y)$ is the propagation function. Convolution by this function represents the effect on the wave function of propagation from one of the scattering planes to the next over a distance $R_1 = R_2 = \ldots R_{N-1}$. The effect of each scattering plane on the wave function is given, as before, by multiplication by

$$q_n(x, y) = \exp\{i\sigma\varphi(x, y)\}\,.$$

It may be noted that equation (8) is of a more general form than the equivalent expressions previously used, for example, in I, since the propagation function is not limited to that appropriate to the paraboloidal approximation to spherical wave fronts. The function $p_1(x, y)$ may be taken as that appropriate to spherical wave fronts including obliquity factors. The only restriction which we place on it is that it must have radial symmetry about the origin.

A straightforward argument then gives the result that $\psi(x, y)$ must have the same symmetry as the $\varphi_n(x, y)$. Thus, the function $q_1(x, y)$ corresponding to the first layer must from its definition, have the same symmetry as $\varphi_1(x, y)$. Convolution of this function with the radially symmetric function $p_1(x, y)$ will change the phase and amplitude distribution around the peaks but not the symmetry. Similarly multiplication by the function $q_2(x, y)$, identical with $q_1(x, y)$, will not affect the symmetry; nor will any of the operations of convolution and multiplication involved in the calculation of $\psi(x, y)$ from equation (8). The argument may be intuitively more obvious for the case that the $\varphi_n(x, y)$ are composed of isolated, radially symmetric peaks. Then convolution with the radially symmetric $p_n(x, y)$ and multiplication by the identical functions $q_n(x, y)$ will change the amplitude and phase distributions of the peaks but not the coordinates of the points about which they are radially symmetric. The wave function on the exit face, $\psi(x, y)$ will therefore have radially symmetric peaks in exactly the same positions as, though of more complicated form than, the peaks of the function $\varphi_n(x, y)$ and so must have exactly the same symmetry.

The diffraction pattern corresponding to $\psi(x, y)$, which is the pattern given by dynamic diffraction for an arbitrary thickness H, will therefore have the same symmetry and the same absences as the planar section of the reciprocal lattice space which corresponds to the diffraction pattern given kinematically by the distribution $\varphi_n(x, y)$. Hence, if the electron beam is exactly parallel to a principal axis of the crystal, no forbidden reflections can be generated by dynamic scattering.

These arguments do not, of course, apply under the conditions for which, for example, the forbidden (222) reflection from the diamond-type lattice has been shown theoretically and in practice to appear. In such cases the incident beam is not parallel to a principal crystal axis and the repetition distance (the effective unit cell dimension) in the beam direction, is then very large and the approximations we have made break down. Our arguments apply strictly only when the beam direction coincides exactly with the crystal axis. It is to be expected that the forbidden reflections will be absent only for a narrow range of beam orientations. A rough estimate of the width of this range may be obtained as follows.

A slight misorientation of the beam is equivalent to a slight progressive displacement of the origins of the functions $q_n(x, y)$ as n increases, the displacement of the origin of $q_N(x, y)$ relative to that of $q_1(x, y)$ being αH, when α is the angular deviation from the exact orientation. In $\psi(x, y)$ therefore, there will be a complicated distribution of peaks along a line of length αH, instead of a single radially symmetric peak, for each atomic peak in the projection $\varphi_n(x, y)$. If the length αH of this line of peaks is much less than the average distance between atom peaks in $\varphi_n(x, y)$, very little interaction of the various peaks will occur and it will be possible to express $\psi(x, y)$ in the form $\varphi_n(x, y) * w(x, y)$, where $w(x, y)$ is some complicated 'peak function'. The diffraction pattern can therefore be written

$$U(h, k) = E_n(h, k) . W(h, k) ,$$

where $E_n(h, k)$ and $W(h, k)$ are the Fourier transforms of $\varphi_n(x, y)$ and $w(x, y)$ respectively. Then if reflections are forbidden kinematically so that $E_n(h, k) = 0$, we have also $U(h, k) = 0$.

If the lines of peaks of length αH overlap appreciably it will not be possible to express $\psi(x, y)$ as a convolution, and the forbidden reflections may occur. The deviation in orientation for which it may be expected that forbiddens will appear is thus of the order given by $\alpha H = b$, the average distance between atomic peaks in the projections $\varphi_n(x, y)$. For example, if $H = 500$ Å, $b = 1{\cdot}5$ Å, we get a critical misorientation of $\alpha \approx 3 \times 10^{-3}$ radians.

Such a misorientation is of the same order as that required to introduce appreciable differences in the observed intensities of symmetrically-equivalent diffraction spots because the Ewald sphere passes at differing distances from the corresponding reciprocal lattice points. If therefore a perfect crystal gives a spot pattern in which the intensity distribution does not appear to be made unsymmetrical by a tilt of the crystal, dynamic diffraction effects cannot give appreciable intensities to any forbidden reflections. If forbidden reflections do appear under such circumstances, it is necessary to find some alternative explanation such as the occurrence of the so-called 'secondary elastic scattering' by crystals containing defects.

4. Diffraction by imperfect crystals

The crystals which have been investigated in connection with single-crystal structure analysis by electron diffraction methods have almost invariably shown evidence of considerable imperfection. Since most of these crystals have been of the layer-lattice type, the predominating form of defect is the stacking fault in which adjacent layers are relatively displaced by a translation which is not made up of integral multiples of unit cell translations. The kinematic theory of diffraction from crystals containing stacking faults has been developed by many authors in connection with X-ray diffraction experiments, but usually with the assumption that the number of faults is sufficiently large to allow statistical methods to be used. For crystals with thicknesses of the order which would make the use of kinematic diffraction theory valid in electron diffraction work, such an assumption cannot be made unless the average distance between stacking faults is very small (i.e., only a few Å), since the total crystal thickness must not exceed a few hundred Å.

Provided that the kinematic theory of diffraction can be considered as a valid approximation, the distribution function method of analysis (Cowley, 1957) can be used to treat crystals with any number of stacking faults. Thus, the projection of the potential distribution, $\varphi(x, y)$ may be expressed in the form

$$\varphi(x, y) = \varphi^0(x, y) * D(x, y) , \quad (9)$$

where $\varphi^0(x, y)$ is the projection of the potential distribution function of an individual layer of atoms and $D(x, y)$ is a distribution function consisting of a set of variously weighted δ-functions. By taking the Fourier transform of (9) we obtain the reciprocal space relationship

$$E_{hk0} = E^0_{hk0} . C_{hk0} , \quad (10)$$

where E^0_{hk0} is the structure factor for a perfect crystal and C_{hk0} is the value of the Fourier transform of $D(x, y)$ at the point $h, k, 0$.

It may be noted that if E^0_{hk0} is zero, E_{hk0} must be zero. Thus forbidden reflections cannot be produced as a result of purely translational displacements of parts of the crystal so long as the kinematic approximation is valid. We illustrate this point by reference to the orthorhombic form of paraffin hydrocarbons examined by electron diffraction methods, for example, by Cowley, Rees & Spink (1951). Single-crystal patterns may readily be obtained with the incident beam parallel to the c-axis. The relevant projection of the structure is then that shown in full lines in Fig. 4. Screw axes parallel to the a and b axes of the structure result in the extinction of the $h00$ and $0k0$ reflections for h or k odd. If now part of the crystal is translated so that the projections of the atoms take the positions shown dotted in Fig. 4, the symmetry of the projection $\varphi(x, y)$ will be changed. The screw axes parallel to the a and b axes are no longer evident. However the projection of the structure on either the *a* or *b* axes still shows a periodicity of half the unit cell edge. Hence, although the intensities of the permitted reflections will be greatly affected, the odd-order *h*00 and 0*k*0 reflections will remain forbidden.

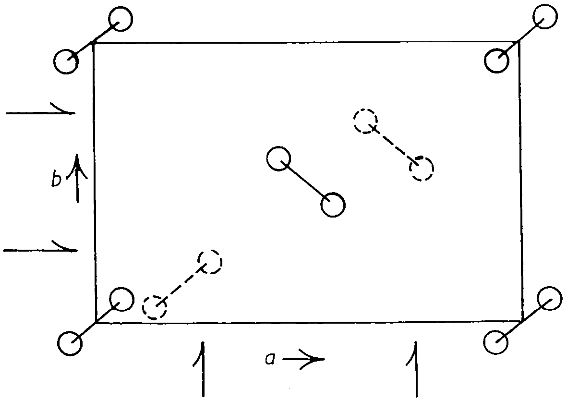

Fig. 4. The projection along the *c*-axis of the structure of orthorhombic crystals of long-chain *n*-paraffins (full lines). The dotted lines indicate the same projection shifted by an arbitrary displacement.

The range of validity of the kinematic theory is usually greater for disordered than for ordered crystals. This is clearly seen if we consider only the first-order approximation used in section 2 above. In this approximation the maximum deviation from the region of validity of the kinematic theory depends on the maximum value of the projection $\varphi(x, y)$ of the potential distribution. When stacking faults occur, the number of atoms directly in line in the beam direction is in general decreased, so that the maximum value of $\varphi(x, y)$ decreases. In this way a single stacking fault near the centre of the crystal can reduce the maximum value of $\varphi(x, y)$ by a factor of about 2.

Under such circumstances the effects of multiple elastic scattering become more important in limiting the range of applicability of the kinematic theory. The diffraction effects may then be formally expressed by taking the Fourier transform of the wave function at the exit face given by equation (8) with appropriate $q_n(x, y)$ functions. Calculations for specific cases could be made with any required degree of accuracy by approximating to (8) by the methods previously mentioned, but no such calculations will be made here. However, some general conclusions may be drawn concerning the appearance of forbidden spots from arguments similar to those used in section 3 above. Thus if two layers of the crystal mutually displaced, are separated by an appreciable distance in the beam direction, the atomic peaks due to the first layer will be broadened by Fresnel diffraction effects (i.e., by convolution with the propagation function) and may overlap, and interact with, atomic peaks due to the second layer. The effects of such overlapping will not have the symmetry of either individual layer, as can be seen from Fig. 4 if interactions are imagined between closest pairs of projected atomic peaks. Hence it will not be possible to express the wave function on the exit face by a convolution such as in equation (9), and forbidden reflections may appear with appreciable intensity. The strength of the forbidden reflections will obviously be dependent on the frequency and nature of the stacking faults.

It may be noted that forbidden reflections may be generated in other ways by crystal defects of different character. For example if there is a slight rotation of one portion of a crystal with respect to another part about an axis in the beam direction, the two crystal regions will give diffraction spots which do not coincide exactly. Because the electron sources used in practice are usually of finite size and almost completely incoherent the diffracted beams from the two crystal portions will not act as if coherent, even though the separation of the diffraction spot centres may be very small compared with the spot size. If then beams are diffracted successively by the two crystal portions, the doubly-diffracted electron beams will behave as if incoherent with each other and with the once-diffracted beams even though the assembly of singly- and doubly-diffracted beams falling around a perfect-crystal spot position gives rise to a diffraction spot only slightly larger than the spot given by a perfect crystal. In particular a forbidden reflection *hkl* will appear with an intensity given by the sum of the intensities of beams doubly diffracted by pairs of planes with indices h_1, k_1, l_1 and h_2, k_2, l_2 such that $h_1+h_2 = h$, $k_1+k_2 = k$ and $l_1+l_2 = l$. In this way the effect of incoherent secondary elastic scattering can be produced. It seems probable that this was the case for the single-crystal patterns from the paraffin dicetyl obtained by Cowley, Rees & Spink (1951). The assumption of incoherent secondary elastic scattering was therefore made the basis of a method for the correction of the intensities of the reflections in a single crystal spot pattern and appeared to give satisfactory results.

5. Conclusion

In this paper we have considered some of the more obvious and direct implications of the new approach to electron diffraction theory introduced in I. We have used for the most part, only first-order approximations and qualitative arguments. More quantitative results can be obtained for particular cases. The accuracy of the results, and the amount of computation involved will increase as higher order approximations are taken.

It has been shown that no forbidden reflections can appear as a result of dynamic scattering in the symmetrical spot patterns given by perfect single crystals when the electron beam is parallel to a principal crystal axis. Dynamic scattering may, however, give rise to forbidden reflections in patterns from perfect crystals with markedly unsymmetrical intensity distributions, in the extensive spot patterns from bent crystals and in powder patterns.

Our arguments have indicated that the range of crystal thickness for which single-crystal structure analysis is feasible is not limited to the range of validity of the kinematic theory as defined, for example, by the calculations of Blackman (1939) for perfect crystals. If the crystals are perfect, the use of our first-order approximation not only allows crystal structure analysis to be carried out for crystals of greater thickness but provides a technique for the unambiguous determination of crystal structures which involves, in effect, the determination of the relative phases of reflections from series of diffraction patterns obtained with different crystal thicknesses or accelerating voltages. If the crystals are imperfect, it has been shown that the range of validity of the kinematic theory is extended. For both perfect and imperfect crystals it seems probable that the use of higher-order approximations, involving the effects of Fresnel diffraction within the crystal, may extend the range of thickness still further although making the mathematical treatment of the diffraction observations much more cumbersome and requiring more detailed knowledge of crystal thickness and imperfections.

References

Blackman, M. (1939). *Proc. Roy. Soc.* A, **173**, 68.
Cowley, J. M. (1953). *Acta Cryst.* **6**, 516.
Cowley, J. M. (1957). *Acta Cryst.* **10**, 141.
Cowley, J. M. & Moodie, A. F. (1957). *Acta Cryst.* **10**, 609.
Cowley, J. M. & Moodie, A. F. (1958). *Proc. Phys. Soc.* **71**, 533.
Cowley, J. M. & Moodie, A. F. (1959). *Acta Cryst.* **12**, 353.
Cowley, J. M., Rees, A. L. G. & Spink, J. A. (1951). *Proc. Phys. Soc.* A, **64**, 609.
Glauber, R. & Schomaker, V. (1953). *Phys. Rev.* **89**, 667.
Heidenreich, R. D. (1950). *Phys. Rev.* **77**, 271.
Ibers, J. A. & Hoerni, J. A. (1954). *Acta Cryst.* **7**, 405.
Schomaker, V. & Glauber, R. (1952). *Nature, Lond.* **170**, 290.

Acta Cryst. (1959). **12**, 367

The Electron-Optical Imaging of Crystal Lattices

By J. M. Cowley

Division of Chemical Physics, Chemical Research Laboratories, Commonwealth Scientific and Industrial Research Organization, Melbourne, Australia

(*Received* 7 *July* 1958)

The theory of the scattering of electrons by crystals previously developed (Cowley & Moodie, 1957*a*) is applied to determine the nature of the image of a crystal lattice obtained with an ideal electron microscope, both in- and out-of-focus. For very thin crystals the pseudo-kinematic theory is applied, and for thick crystals the dynamic theory in a two-beam approximation is used. Intensity anomalies and 'stepped' structures in micrographs showing the 90 Å superlattice spacing of a form of antigorite are explained as arising from simultaneous dynamic scattering of a fundamental lattice reflection and kinematic scattering of the superlattice reflection.

It is shown that dynamic scattering can give rise to variations in the spacing and orientation of moiré-like fringes appearing in electron microscope images of superimposed crystals.

1. Introduction

In recent years a number of observations have been made of periodic intensity modulations of electron microscope images of thin crystals, the periodicities corresponding to the separations of prominent lattice planes of the crystals. The crystals concerned include metal phthalocyanines, (Menter, 1956*a*; Neider, 1956; Suito & Uyeda, 1957) faujasite (Menter, 1956*b*) and molybdenum trioxide (Bassett & Menter, 1957). The periodicities observed for these compounds corresponded to spacings of less than 20 Å and have been interpreted as given by interference of the first one or two diffracted beams with the transmitted beam, probably with changes of the relative phase of the interfering beams due to the spherical aberration of the objective lens.

On the other hand, several observations have recently been made of much larger periodicities, of the order of 100 Å, in which case it seems likely that the interference of the electron beams corresponding to at least the first few diffraction orders should not be seriously affected by lens aberrations. Examples include periodicities of about 40 and 90 Å observed in samples of antigorite by Brindley, Comer, Uyeda & Zussman (1958). Similarly, for the moiré-like fringes which appear in the electron microscope images of